COMPOSITION OPTIMIZATION OF ZEOTROPIC MIXTURES FOR ORC SYSTEMS CONSIDERING CONSTRAINTS

Benedikt Gregor Bederna[1]*, Riley Bradley Barta, Ullrich Hesse

[1]Bitzer-Professur für Kälte-, Kryo- und Kompressorentechnik,
Technische Universität Dresden, 01062 Dresden, Germany

* Corresponding Author: benedikt.bederna@tu-dresden.de

ABSTRACT

Organic Rankine Cycle (ORC) processes are used to convert low-temperature waste heat into electricity. Often, these sources and sinks are sensible heat flows. In such a case, it may be appropriate to adapt the cycle process to these external temperature characteristics. This can be realized with zeotropic mixtures as a working fluid and evaluated by an exergy calculation and the exergetic efficiency. In addition to the usual degrees of freedom for the optimization of conventional ORC processes, the composition of the mixture is therein also a varying parameter. This depends on the predefined parameters of the source and sink, such as the mass flows or outlet temperatures of the system, as well as the outlet power or auxiliary power consumption of the components. Particularly in small-scale systems, the economic aspects play an overriding role so that constraints such as the minimal power density or maximum volume flow rates of volumetric expanders should be included in the optimization process. For this purpose, a two-stage optimization tool is presented which determines the optimal composition for up to quaternary mixtures and takes constraints of the source, the sink, and components used into account. In a time-saving analytical pre-calculation, the process can already be optimized and parametric studies or initial value variations can easily be carried out. The results serve as input parameters for a numerical post-calculation, which models the cycle in detail and performs further optimization. The functionality of this tool is illustrated by means of an ORC system with an air-cooled condenser at a sensible waste heat source temperature of 90 to 120 °C and initial results and observations are presented. Two mixtures with the respective preselected components R-1234ze(E), R-1224yd(Z), R-1233zd(E) and R-1336mzz(Z) as well as R-290, R-600a, R-600 and R-601 are used for this purpose. It was proven that higher exergetic efficiencies and net power can be achieved through application of zeotropic mixtures, but the component limitations, such as condenser geometry and pressure losses, have serious influences on the optimal composition and concentration of the mixtures.

1 INTRODUCTION

The central response to global climate change is the restructuring of the energy and industrial sectors with the aim of achieving an emission-free supply of energy and goods. In this context, regenerative energy sources and the efficient design of industrial processes are particularly in focus. As a simple and robust technology for the conversion of low-temperature heat flows in a wide power range, the Organic Rankine Cycle (ORC) process will play an increasing role in this context. In order to improve the economy, efficiency and application range of this process, the use of zeotropic mixtures has been intensively investigated for years as summarized by Miao *et al.* (2018). The specific motivations for the use of zeotropic mixtures, which exhibit a temperature change during the phase change, can be quite different. Frequently, the reduction of exergy losses in the heat exchangers is named as a goal. Also, a better adaptation to the heat supply of source and sink, combined with a better source utilization can be the background (Lecompte *et al.*, 2014). Under certain circumstances, the electrical energy consumption of auxiliary consumers, such as the brine pump or fans, can also be reduced by the application of zeotropic mixtures, or concrete outlet temperatures of the heat source and sink are required. The central challenge in the design of such processes is to identify the mixture composition that best meets the

optimization criteria. This task is much more complex compared to process optimization for pure working fluids, and the complexity increases as the number of components increases. However, a pure consideration of binary mixtures as shown by Huster *et al.*, 2020 is not sufficient for large temperature glides, since binary mixtures in the two-phase region often form strong nonlinear temperature curves, which are usually disadvantageous. By adding a third or even a forth mixture component, this glide can be linearized or adapted to a desired shape while fulfilling the former thermodynamic requirements. With respect to ternary mixtures, a high number of local optima can occur and the identification of a global optimum is accompanied by increased mathematical complexity. For near-industry design tasks, the long computation times or the high complexity of the optimization models may also be a drawback. The goal of this work is to provide a comparatively simple optimization calculation for the concentration of up to quaternary mixtures for a subcritical ORC process, taking into account constraints of the source, sink, and components used. This is particularly important with the recent trend towards smaller modular ORC systems (20 to 500 kW_{el}), which are mainly built from standard components from other industries (especially refrigeration) due to economic considerations. Preferably, these systems are directly ambient air cooled to make installation and operation simple, cost effective and flexible. Due to the challenge of economic operation despite small power outputs and the predetermined application limits of the standard components, the optimization of the mixture composition is not free here, but is dominated by the constraints. For volumetric expanders in particular, constraints such as the volume ratio and the volumetric power density play a significant role. Standard expanders derived from compressors have predefined volume ratios. Regarding the power density, the rotation speed cannot be easily increased and size scaling is only possible at substantial additional cost. Thereby the optimization of the fluid composition in the field of volumetric expanders has a large potential to achieve significant improvements in net power output. These economic, technically practical and energetic aspects of an application-oriented design are to be met with this optimization model.

2 MODEL DISCRIPTION

2.1 Field of application

The developed model is designed for ORC plants with a simple structure of four main components and for subcritical processes (Fig.1). The condenser is assumed to be a heat exchanger cooled by ambient air with its own fans, which can be specified as either cross-flow or counter-flow. However, due to its modularity, the model can also be equipped with additional components such as piping or a recuperator can be adapted to other circuits and process architectures. It allows minimizing or maximizing of any process parameter, for example the efficiencies, energy flows or the heat exchanger surfaces, while varying the pump and expander inlet pressures and the concentrations of up to four single components of the working fluid mixture. Constraints can be operating limits of the components such as the minimum or maximum pressures, flow volumes, heat exchanger surface area or pressure ratios as well as the conditions of the source and sink such as energy flow and the outlet temperatures.

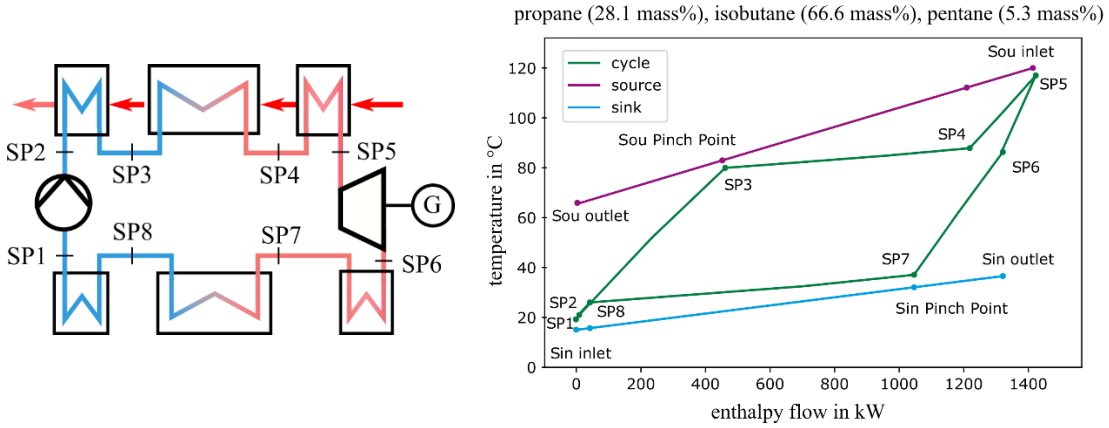

Figure 1: Simplified structure and exemplary T, $\dot{H}$-diagram of the assessed ORC systems

2.2 Program Structure

The model was implemented in the Python programming language. An import and export interface with Excel facilitates the input and evaluation of many parallel comparison calculations. The fluid data for the calculations are taken from the fluid property library REFPROP 10.0 (Lemmon *et al.*, 2018) and integrated via the low-level interface of CoolProp (Bell *et al.*, 2014). This minimizes the computational time needed to access the property database. The cycle is modeled using state points, which contain the respective thermodynamic parameters like the temperature, pressure, enthalpy and less-tangible parameters such as the exergy or the Carnot factor. The individual components can be discretized according to the desired level of detail by means of sub-elements, thus resulting in an arbitrary number of state points within the component. The model is designed in two stages and consists of an analytical pre-calculation and a numerical post-calculation. In the preliminary calculation, the process can already be optimized, but pressure losses or further details cannot be represented. Due to the time-saving step-by-step analytical identification of the state points, extensive parametric studies or initial value variations can easily be carried out with a short runtime in the first stage. The results subsequently serve as input values for the second numerical detail optimization. This can significantly reduce the computation time of the second stage. The numerical post-calculation stage is based on the work of Savelyeva *et al.* (2018). The solvers of the SciPy library (1.5.2) *COBYLA*, *SLSQP*, and *hybr* are used to perform the solution of the optimization tasks and equation systems that arise.

2.3 Calculation Method

In the expander, irreversibilities are taken into account in the form of an isentropic efficiency (Eq. 1). Furthermore, a fixed pressure ratio or a volume ratio can optionally be specified. In this case, the change of state in the expansion machine is divided into an expansion and an expulsion process. The state point SP6' is introduced as the state after expansion and before discharge from the expander itself. The pre-outlet, or over-expansion, of the vapour is taken into account when determining the total work (Eq. 2).

$$\eta_{is} = \frac{w_t}{w_{t,is}} = \frac{(h_{out} - h_{in})}{(h_{is,out} - h_{in})} \tag{1}$$

$$W_t = \frac{[h_{SP5} - h_{SP6'} + v_{SP6'} \cdot (p_{SP6'} - p_{SP6})] \cdot \dot{m}_{cycle}}{\eta_{is}} \tag{2}$$

The simplest way to determine the required fan power is through Eq. 3 based on the air volume flow, the air-side pressure drop in the condenser, the fan efficiency and the efficiency of its motor an power electronics.

$$P_{el,fan} = \frac{\dot{V}_{air} \cdot \Delta p_{air}}{\eta_{fan} \cdot \eta_{fan,motor,PE}} \tag{3}$$

For each state point of the model, the exergy flow is also calculated as a thermodynamic pseudo-parameter according to Eq. 4. The ambient temperature and the ambient pressure serve as a reference. The difference between these pseudo-parameters can then be used to determine the exergetic losses of each component. Thus, the exergetic losses of the pump are determined exemplarily via Eq. 5. The exergetic efficiency, which is normally used for optimization, is determined by the net power and the input energy flow of the heat source (Eq. 6).

$$\dot{E}_{SP} = \dot{m}_{SP} \cdot [h_{SP} - h_{amb} - T_{amb} \cdot (s_{SP} - s_{amb})] \tag{4}$$

$$\dot{E}_{loss,pump} = \dot{E}_{out} - \dot{E}_{in} - P_{el,pump} \tag{5}$$

$$\eta_{exergetic} = \frac{P_{el,net}}{\dot{E}_{sou,in}} \tag{6}$$

2.4 Comparison of Heat Exchanger Design

The calculation of the heat exchangers can be done in a simple way using either a minimum temperature difference method or a surface area and a heat transfer coefficient method. In the case of the second method, suitable k-values have to be predefined in this model by the user themselves, because it is not the aim to define the detailed heat exchanger geometry in advance. Based on the findings of Weith et al. (2014), it is recommend to define the k-value for a mixture as the lowest k-value of the single mixture components. However, if the heat exchanger design deviates from the direct counter-flow or the parallel-current principle, such a calculation is no longer useful since the minimum temperature difference and the average logarithmic temperature difference cannot be easily determined. Therefore, it is intended to calculate the heat exchangers by means of a Number of Transfer Units (NTU) value, as outlined in the VDI-Waermeatlas (VDI, 2013). Since chillers in practice often use heat exchangers with a cross-flow geometry, a comparison of both heat exchanger geometries is inevitable. In this case, a design calculation is first carried out in this work using the minimum temperature difference and counter-flow geometry for each individual discrete heat exchanger element and the NTU value is determined for each according to Eq. 7. This value then serves as an input variable for Eq. 8 (VDI, 2013, p. 47), which describes the new and smaller dimensionless temperature change (Eq. 9) of the ideal cross-flow. Thus, a determination of the new required air mass flow and associated volume flow as well as the fan power (Eq. 3) can be made via the capacity flow ratio (Eq. 10).

$$\mathrm{NTU} = \frac{k \cdot A}{c_p \cdot \dot{m}} = \frac{k \cdot A}{\dot{Q}/(T_{out} - T_{in})} \tag{7}$$

$$P_i = \frac{1}{R_i \mathrm{NTU}_i} \sum_{m=0}^{\infty} \left\{ \left[1 - e^{-\mathrm{NTU}_i} \sum_{j=0}^{m} \frac{1}{j!} {\mathrm{NTU}_i}^j \right] \left[1 - e^{-R_i \mathrm{NTU}_i} \sum_{j=0}^{m} \frac{1}{j!} (R_i \mathrm{NTU}_i)^j \right] \right\} \tag{8}$$

$$P_{air} = \frac{T_{in,air} - T_{out,air}}{T_{in,air} - T_{in,cycle}} \tag{9}$$

$$R_{air} = \frac{c_{p,air} \cdot \dot{m}_{air}}{\dot{Q}_{cycle}/(T_{out,cycle} - T_{in,cycle})} \tag{10}$$

2.5 Optimization Process Monitoring

If the composition of three or more components is to be optimized, several concentration combinations with similar resulting variables occur. These are local optima, which in most cases are close to the global optimum. From a mathematical point of view, a global optimization is not performed with the calculation model in its current state. However, since practical technical considerations are in the foreground for this optimization application, this does not necessarily have to be striven for in this preliminary investigation. Once the various optima have been identified, they can be examined for favourable combinations of process properties. An initial value variation for the analytical pre-calculation has proved successful, in which the concentration fractions can be set from 10 % to 70 % at 20 % intervals for each component. This results in 20 possibilities, which should be supplemented by the four pure substances. However, the greatest challenge in continuous optimization is undefined areas in the mixture properties. Especially for hydrofluoroolefins (HFO) and alkenes, the mixture models and estimations contain various uncertainties and points of discontinuity. These result in less reliable optimization results and numerical challenges, which is why a sophisticated numerical exception handling strategy is of utmost importance.

3 CALCULATION RESULTS

In the following section, the developed model will be applied to individual examples to illustrate the influence of the component limitations, the condenser design and the pressure losses on the optimization of quaternary mixtures. For this analysis, a simple ORC system composed out of industrial standardized components (pump, heat exchanger) and a volumetric expander adopted from the refrigeration sector is considered. This is currently a fast growing market of ORC systems and the optimization process includes various constraints. The selected source temperature study range is from 90 °C to 120 °C with an ambient air temperature of 15 °C. A fixed generator design power of 100 kW_{el} is optimized according to the exergetic efficiency. Mixtures consisting of up to four promising working fluids, which are either hydrocarbons or HFOs, are investigated. All key aspects and assumptions of the following calculations are summarized in Table 1. The assumptions made are in line with values commonly used in the literature for systems of this power range equipped with a volumetric expander.

3.1 Effect of Constraints

For ORC systems composed of standardized or adopted components, the predefined component limitation plays a significant role. To represent this, five common constraints that can occur in pumps and volumetric expanders were selected (Table 2). The two quaternary mixtures are each optimized analytically in the temperature range, once with and once without these limitations, to illustrate their effect. The results of the optimized mixtures are compared with an ORC process using the particular pure fluid of the mixture with the highest volumetric power density. Only R-1234ze(E) and propane can meet the demanding ratio of generator power to expander inlet flow volume of 0.374 $kW \cdot hr \cdot m^{-3}$ throughout the entire temperature range.

Table 1: Input parameter for thermodynamic calculations

Parameter	Value
Pre-selection of potential hydrofluoroolefins (HFO)	R-1234ze(E), R-1224yd(Z), R-1233zd(E), R-1336mzz(Z)
Pre-selection of potential hydrocarbons (HC)	propane, isobutane, n-butane, n-pentane
Heat source temperature (pressurized water)	90 - 120 °C
Heat sink temperature (air)	15 °C
El. generator power	100 kW
Expander isentropic efficiency	0.7
Expander and generator efficiency (mechanical)	0.98, 0.98
Generator and power electronics efficiency (electrical)	0.92, 0.96
Pump isentropic efficiency	0.7
Motor and power electronics pump efficiency	0.9
Pressure drop condenser air side	100 Pa

Table 2: Selected component constraints

Parameter	value
Minimal subcooling (cavitation limit)	6 K
Maximal absolute pump pressure (pressure limit)	2.5 MPa
Maximal pump pressure rise (bearing limit)	1.2 MPa
Maximal expander inlet volume flow (rotation limit)	288 m^3/h
Build-in expander volume ration (geometric limit)	3

In all calculated cases with constraints, the volume flow limit of the expander comes into play. The optimum exergetic efficiency would always occur at either higher expander volume flows or lower evaporation pressures, respectively. For the hydrocarbon mixtures, the pressure rise of the pump still

always represents a limit. In the case of the HFOs, this only applies to the pure substance R-1234ze(E). At a source temperature of 90 °C, the volume ratio of the expander is too large for both groups of working fluids, resulting in overexpansion. With regard to the optimum composition determined, it is initially striking that none of the maximum quaternary mixtures actually consists of four components. For the HFOs, a ternary mixture of R-1234ze(E), R-1233zd(E) and R-1336mzz(Z) is obtained for the unconstrained case without component limitations, and only a binary mixture of R-1234ze(E) and R-1336mzz(Z) for the constrained case (Figure 2). No butane is used for the hydrocarbons mixtures in each case (see Figure 1). The composition of the two working fluids differs greatly between the unconstrained and constrained cases. For both mixtures the share of the fluid composition with the highest volumetric power density (R-1234ze(E), propane) is larger in the constrained cases in order to fulfil the limitation of a maximum expander inlet volume flow. For an increasing source temperature, the fluid composition with the highest volumetric power density decreases in order not to exceed the pressure limits (Figure 2, right). The concentration of a single component over the temperature range can vary by up to 24 % (propane, unconstrained case).

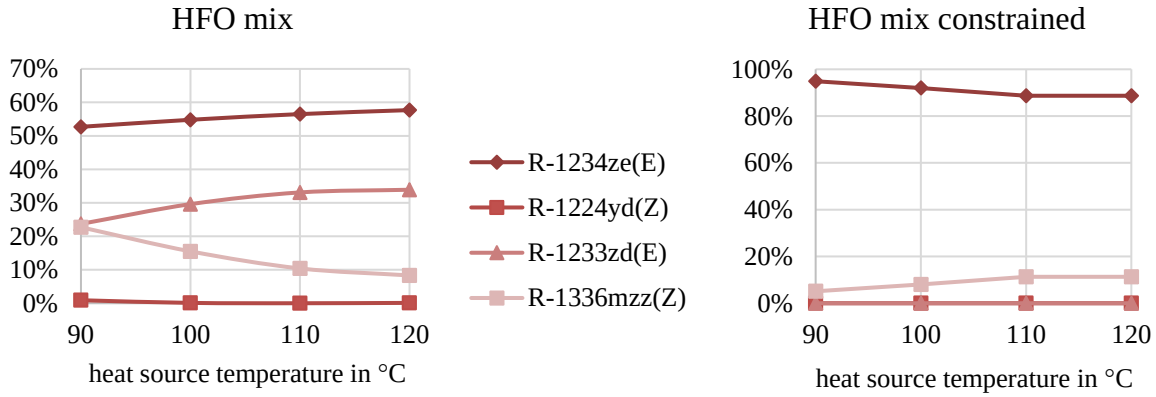

Figure 2: Composition of the optimal working fluids composed out of HFOs for the unconstraint (left) and the constrained case (right)

The points of the optimized exergetic efficiencies, which are each related to a specific composition, are shown in Figure 3. The values indicate a significant improvement over the pure substance in the unconstrained case, especially at low temperatures. Even for the constrained scenario, a small improvement exists.

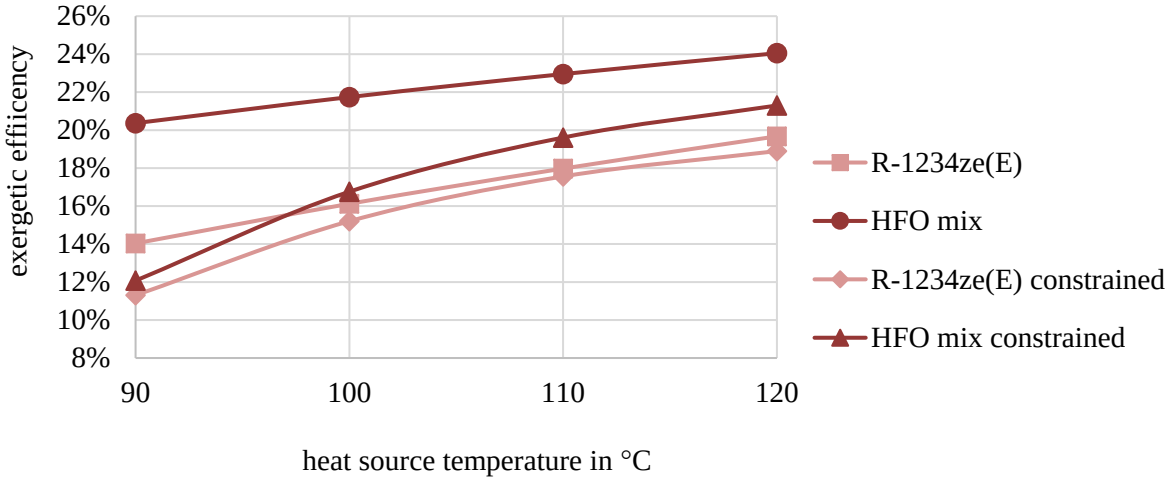

Figure 3: Comparison of efficiencies for the working fluid group of HFOs

However, this observation should be evaluated rather qualitatively, since a specific optimization of the pure substance selection for each temperature level did not take place. The efficiency curves of the hydrocarbons behave similarly to those of the HFOs, but they are slightly (on average 4.4 %) lower.

For the net power output at the point of optimal exergetic efficiency a strong improvement can be observed in all categories (Figure 4). The apparent advantages of the hydrocarbon mixtures are caused by the higher source mass flow, which leads to the lower exergetic efficiencies in the case of the hydrocarbon mixtures. If the identical source mass flow as was observed with the HFO mixtures is applied, the performance of the hydrocarbons is slightly lower than that of the HFOs (except for two points). It is encouraging to observe that the mixtures cause the net power to drop less at lower temperatures. This may contribute to the expansion of the economic range of application toward lower source temperatures.

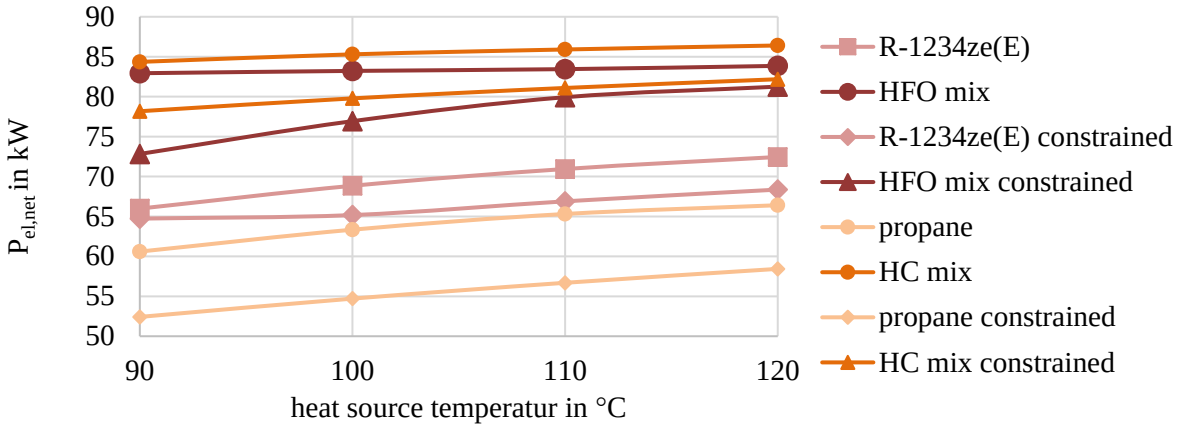

Figure 4: Comparison of the net power outputs at the respective optimal exergetic efficiencies

3.2 Comparison of Counter- and Cross-Flow Heat Exchanger Geometries

A comparison of the different condenser geometries was carried out for the unconstrained case at a source temperature of 90 °C. As shown in Figure 5, this also has a direct influence on the composition of the optimum mixture and, in particular, on the shape of the isobars in the two-phase region.

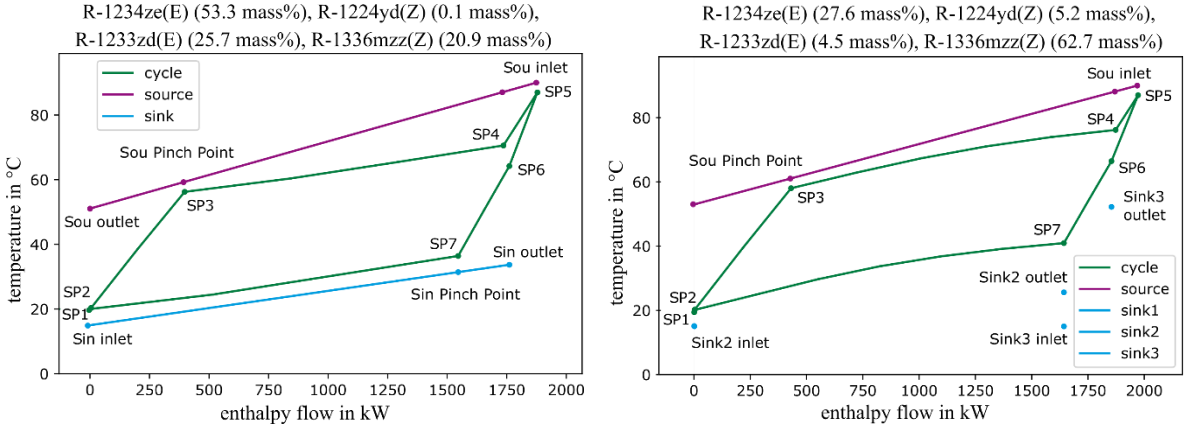

Figure 5: *T*-$\dot{H}$-diagrams of optimized, unconstrained ORC processes using a condenser with a counter-flow (left) and a cross-flow geometry (right) with the indicated average outlet temperatures of the two condenser sections at a heat source temperature of 90 °C

Whereas with counter-flow condensers the phenomenon can be observed that the condensation curve is fitted to the cooling water characteristic, which thus usually corresponds to a linear curve or a small bowed outward curve (slightly visible in Figure 1), the inverse behaviour occurs with a counter-flow condensers. Then, the profile of the evaporation is adapted to the source profile so that, consequently, condensation can take place in the condenser in large surface fractions at high temperatures. The result is also a high sink outlet temperature at the respective points and thus a lower required volume flow and smaller fan power. In this case, it can further be illustrated that the improvement in exergetic efficiency and corresponding net power by a mixture is lower when using the cross-flow geometry. For the counter-flow geometry, there was an increase from 14.3 % to 20.4 % and 71.3 kW to 82.7 kW, and, for

the cross-flow geometry, the increase was smaller, achieving an increase from 14 % to 16.5 % and 69.2 kW to 74.1 kW.

3.3 Effect of Pressure Drops

Finally, the influence of the pressure losses occurring in the cycle on the optimal mixture composition will be discussed. For this purpose, pressure losses for the individual components were assumed (Table 3) based on research conducted on available industrial plate and finned tube heat exchangers. As an example, the HFO mixture is calculated without component limits.

Table 3: Assumption of pressure drops

Heat exchanger	Pressure drop external side	Pressure drop cycle side
Preheater + Evaporator + Superheater	19 kPa + 2 kPa + 1kPa	5 kPa + 7 kPa + 4 kPa
Precooler + Condensator + Subcooler	30 Pa + 40 Pa + 30 Pa	30 kPa + 40 kPa + 10 kPa

As expected, the consideration of the pressure losses reduces the exergetic efficiencies and the net power outputs of the cycle, although the effects on the efficiencies are more pronounced in the considered temperature range and lie between -26.4 % and -21.6 %. This is mainly due to the pressure losses in the evaporator. In order to maintain the expander inlet pressure, the evaporation pressure, and thus the evaporating temperature, at the pinch point of the evaporator must be raised. Therefore, the source outlet temperature after the evaporator also rises, which is the reason why the exergetic losses of the heat source increase higher than average. This also affects the choice of the optimal mixture composition. The pressure loss increases the temperature glide in the condenser but reduces it in the evaporator. Due to the described deciding influence of the pinch point, it is not possible to simply set the identical temperature glide in the condenser as in the case without pressure losses. Otherwise, the temperature glide in the evaporator would drop too much and cause unbalanced exergy losses by higher source outlet temperatures. The result of the optimization process, as shown in Figure 6, is therefore a higher temperature glide in the condenser and less reduced temperature glide in the evaporator. Nevertheless these glides are again achieved by the same mixture of R-1234ze(E), R-1233zd(E) and R-1336mzz(Z) with slightly modified compositions. At 90 °C, a flattening of the temperature glide curve can be observed, which is due to the fixed generator power of 100 kW_{el}. In the case without pressure losses, this would occur only at lower source temperatures.

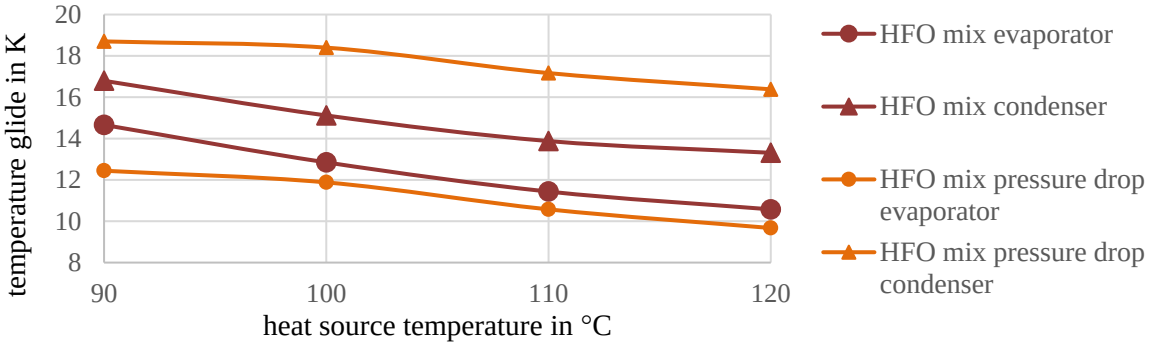

Figure 6: Effect of cycle pressure drops of the optimal temperature glides

4 CONCLUSIONS

In this work a calculation tool for ORC systems was presented, which optimizes processes with up to quaternary mixtures with predefined constraints of the source, sink and components used. The functionality was demonstrated by examining exemplary the effect of the component limits, the condenser geometry and the pressure drop on the composition for an ORC process with a volumetric expander. These first results and observations can be summarized by the following points:

- A process with a zeotropic mixture composed out of the HFOs R-1234ze(E), R-1224yd(Z), R-1233zd(E), R-1336mzz(Z) or the hydrocarbons propane, isobutane, n-butane, n-pentane can achieve higher exergetic efficiencies and resulting net power output than a process using the particular pure fluid of the mixture with the highest volumetric power density (R-1234ze(E), propane). For decreasing source temperatures, this improvement increases.
- When additional component limitations are considered, other working fluid components and concentrations are found to be optimal, but mixtures are still better than pure working fluids. For this study case, the share of the fluid component with the highest volumetric power density is generally higher if the expander inlet volume flow is limited, and decreases with higher temperature to remain within the absolute pressure limits.
- The geometry of the condenser influences the optimal shape of the isobars in the two-phase region. The average condensation temperature in the cross-flow geometry is higher to reduce the air flow needed. For the study case, the mixture could increase the exergetic efficiency from 14.3 % to 20.4 % for the counter-flow geometry and only from 14 % to 16.5 % for the cross-flow geometry. The improvement in net power output for the cross-flow geometry is smaller as well.
- Considered pressure losses in the components reduce the optimal temperature glide in the evaporator and raise the optimal glide in the condenser to achieve optimal exergetic efficiency.
- The determined optimal working fluids were ternary mixtures in the majority of calculated cases, although quaternary mixtures were assessed in the optimization.

NOMENCLATURE

A	heat exchanger surface (m^2)	p	pressure (kPa)
c_p	specific heat capacity (kJ/(kg K))	P	dimensionless temperature difference
$\dot{E}$	exergy flow (kW)	P	electrical power (kW)
η	efficiency	R	capacity flow ratio
h	specific enthalpy (kW/kg)	S	entropy (kJ/K)
$\dot{H}$	enthalpy flow (kW)	T	temperature (K)
k	heat transfer coefficient (W/(m^2 K)	$\dot{Q}$	heat flow (kW)
$\dot{m}$	masse flow (kg/s)	w	specific work (kW/kg)
NTU	number of transfer units	W	work (kJ)

Subscript

air	air flow of condenser	is	isentropic
amb	ambient	PE	power electronics
cycle	working fluid of cycle	SP	state point
el	electrical	t	technical

REFERENCES

Bell, I. H., Wronski, J., Quoilin, S., Lemort, V., 2014, Pure and Pseudo-pure Fluid Thermophysical Property Evaluation and the Open-Source Thermophysical Property Library CoolProp, *Ind. Eng. Chem. Res.*, vol. 53.

Huster, W. R., Schweidtmann, A. M., Mitsos, A, 2020, Globally optimal working fluid mixture composition for geothermal power cycles, *Energy*, vol. 212.

Lecompte, S., Ameel, B., Ziviani, D., van Den Broek, M., de Paepe, M., 2014, Exergy analysis of zeotropic mixtures as working fluids in Organic Rankine Cycles. *Energy Convers. Manag*. 85, p. 727–739.

Lemmon, E.W., Bell, I.H., Huber, M.L., McLinden, M.O., NIST Standard Reference Database 23: Reference Fluid Thermodynamic and Transport Properties-REFPROP, Version 10.0, NIST.

Miao, Z., Zhang, K., Wang, M., Xu, J., 2018, Thermodynamic selection criteria of zeotropic mixtures for subcritical organic Rankine cycle, *Energy*, vol. 167.

Savelyeva, S., Kloeppel, S, Haberstroh, Ch., 2018, CryoSolver, Package for cryogenic cycle simulation in Python. Doc. Ver. 1.0.0. Dresden, https://doi.org/10.5281/zenodo.4001668.

VDI, 2013, VDI-Wärmeatlas, Springer Berlin Heidelberg.

Weith, T., Heberle, F., Preißinger, M., Brüggemann, D., 2014, Performance of Siloxane Mixtures in a High-Temperature Organic Rankine Cycle Considering the Heat Transfer Characteristics during Evaporation. *Energies*, vol. *7*.

ACKNOWLEDGEMENT

The work was carried out within the framework of a project of *Zentrales Innovationsprogramm Mittelstand (ZIM)*, which was funded by the German Federal Ministry of Economics. Thanks to Meike Herold for the helpful exchange and contributions to the analytical calculation of ORC processes in Python.